

# Controlling Quasibound States in 1D Continuum Through Electromagnetic Induced Transparency Mechanism

Z. R. Gong,<sup>1</sup> H. Ian,<sup>1</sup> Lan Zhou,<sup>2,3</sup> and C. P. Sun<sup>1</sup>

<sup>1</sup>*Institute of Theoretical Physics, The Chinese Academy of Sciences, Beijing, 100080, China*

<sup>2</sup>*Department of Physics, Hunan Normal University, Changsha 410081, China*

<sup>3</sup>*Frontier Research System, The Institute of Physical and Chemical Research (RIKEN), Wako-shi 351-0198, Japan*

(Dated: October 28, 2018)

We study the coherent scattering process of a single photon confined in an one-dimensional (1D) coupled cavity-array, where a  $\Lambda$ -type three-level atom is placed inside one of the cavities in the array and behaves as a functional quantum node (FQN). We show that, through the electromagnetic induced transparency (EIT) mechanism, the  $\Lambda$ -type FQN bears complete control over the reflection and transmission of the incident photon along the cavity-array. We also demonstrate the emergence of a quasibound state of the single photon inside a secondary cavity constructed by two distant FQN's as two end mirrors, from which we are motivated to design an all-optical single photon storage device of quantum coherence.

PACS numbers: 42.50.Gy, 32.80.Qk, 03.65.Nk, 42.70.Qs

## I. INTRODUCTION

In recent years, many efforts have been exerted to implement all-optical quantum devices [1, 2, 3, 4] that can coherently control photons through photons [5, 6, 7, 8, 9]. This application-oriented pursuit requires the possible existence of a strong and controllable photon-photon interaction. From the view of modern physics, photons do not couple to each other directly through fundamental electromagnetic interactions; however, people recognized that two photons interact indirectly via nonlinear media [10, 11, 12, 13, 14]. Such nonlinear interactions are usually obtained through high-order perturbation theories and hence cannot be arbitrarily manipulated according to one's will. Nevertheless, inside some artificial medium, the transport of photons can be well controlled by an additional intervening classical field [1].

In this paper, we revisit this problem of photon transportation under a coherent architecture, based on the theoretical approach we have developed in Ref. [15]. We propose that a coupled cavity-array, regarded as an one-dimensional (1D) continuum, provides a transport channel to an incident single photon. Placed inside one of the cavities, a  $\Lambda$ -type three-level atom can either grant or block the path of the single photon by the atom's electromagnetic induced transparency (EIT) effect. This atom can essentially be regarded as a functional quantum node (FQN). In fact, a similar mechanism has been used to build the so-called single-photon transistor, analogous to an electronic transistor in which an atom plays the role of the gate through its absorption and emission of photons to-and-fro a channel [2].

In comparison with the design of the "single-photon transistor", in which the photon travels continuously through a fiber waveguide, our cavity-array lets the photon travel discretely through the channel by locally creating or annihilating a photon between its cavities. We hence consider the coherent scattering process of the pho-

ton with the forementioned FQN in the discrete coordinate representation. Our approach is then a generalization of the 1D process where a photon is scattered by the  $\delta$ -potential set up by a FQN through its EIT effect into the discrete space. Such an approach raises a richer spectrum structure indicated by its nonlinear dispersion relation resulting from the tight-binding inter-cavity coupling, as opposed to the usual linear dispersion relations. Because of the unusual dispersion relation, we develop a new approach for the transport of the single photon, which is different from the effective field approach [16] normally adopted; yet the high energy limit of our setup can cover the main results of the theoretical approaches of similar single-photon transistor designs [16, 17, 18].

We generalize the discrete scattering method recently proposed [15] and calculate the reflection and the transmission coefficients of the single-photon transport as functions of both the Rabi frequency and the level spacing between the excited state and the metastable state of the FQN. The reflection and the transmission spectra of the photon are depicted by general lineshapes whose ranges cover both the high-energy end at the Breit-Wigner limit and the low-energy end at the Fano-Feshbach limit. As emphasized, it is the classical field that control the system to reach such high energy and low energy limits. Our derivations show that the  $\Lambda$ -type FQN can behave as a perfect mirror to totally reflect the incident photon when the Rabi frequency matches the frequency of the controlling classical field. The behavior of the FQN has suggested a basic mechanism to implement all-optical control for single-photon transports and provides the ground for a photon storage device through controllable quasibound states, which are defined in Ref. [19, 20], inside a secondary cavity braced by two distant FQN's.

The rest of the paper is organized as follows. In Sec. II, we present the model Hamiltonian for a single photon scattered by a  $\Lambda$ -type FQN. In Sec. III, we derive the scattering equation for the transport of the single photon

and demonstrate the somewhat equivalent role played by a  $\Lambda$ -type FQN and two two-level FQN's at some particular positions. In Sec. IV, the reflection and the transmission coefficients are derived to find the conditions for perfect reflection and transmission; the spectrum line-shapes at high and low energy limits are also calculated. In Sec. V, we illustrate the mechanism we design for photon storage. The conclusion is given in Sec. VI.

## II. MODEL SETUP

We consider an 1D coupled cavity array, in which the transport of a single photon is described by a bosonic tight binding model. A  $\Lambda$ -type three-level atom, whose ground state, metastable state and excited state are denoted as  $|g\rangle$ ,  $|a\rangle$  and  $|e\rangle$ , respectively, is placed in one of the cavities. A strong classical field with frequency  $\omega_C$  matches to the  $|e\rangle \rightarrow |a\rangle$  transition, while the photon, considered a weak quantum radiation field and traversing in the cavity array with frequency  $\omega_P$ , matches to the  $|e\rangle \rightarrow |g\rangle$  transition. The classical field as the control and the quantum field as the probe dress the three-level atom into an EIT medium. The system and the detailed structure of the EIT medium are shown in Fig. 1(a) and Fig. 1(b), respectively.

The total Hamiltonian

$$H = H_p + H_a + H_c \quad (1)$$

contains three parts, describing in order: the propagation of the photon, the free  $\Lambda$ -type three-level atom, and the controlling couplings

$$H_p = \sum_j [\omega b_j^\dagger b_j - t(b_j^\dagger b_{j+1} + h.c.)], \quad (2a)$$

$$H_a = \omega_e |e\rangle \langle e| + \omega_a |a\rangle \langle a|, \quad (2b)$$

$$H_c = \Omega(e^{-i\omega_C t} |a\rangle \langle e| + h.c.) + g(b_0^\dagger |g\rangle \langle e| + h.c.), \quad (2c)$$

where  $b_j^\dagger$  is the creation operator of photon at site  $j$  with  $\omega$  the cavity field frequency and  $t$  the hopping coefficient;  $\omega_e$  and  $\omega_a$  are the energy level spacings of the metastable state and the excited state, respectively;  $\Omega$  is the Rabi frequency due to the control field and  $g$  the coupling constant to the probe field.

We first consider the scattering process in a ‘‘rotating’’ frame of reference, which is defined by a unitary transformation  $U = \exp(-i\omega_C |a\rangle \langle a| t)$ . Then the original Hamiltonian is changed into a time independent one as

$$\begin{aligned} H^R &= U^\dagger H U - iU^\dagger \partial_t U \\ &= H_p + H'_a + H'_c, \end{aligned} \quad (3)$$

where, corresponding to renormalized  $\Lambda$ -type atom and controlling interaction, respectively,

$$H'_a = \omega_e |e\rangle \langle e| + \Delta |a\rangle \langle a|, \quad (4a)$$

$$H'_c = \Omega(|a\rangle \langle e| + h.c.) + g(b_0^\dagger |g\rangle \langle e| + h.c.). \quad (4b)$$

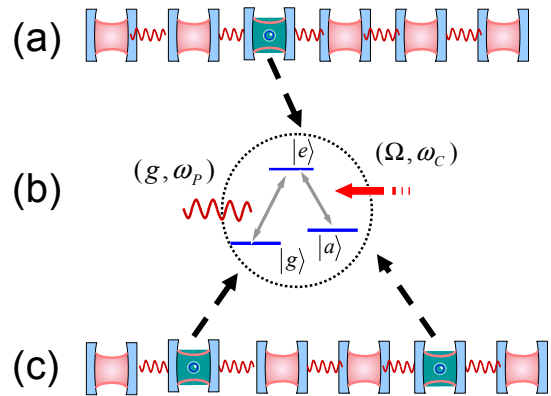


FIG. 1: (Color online) Schematic of the model setup. (a) shows the 1D coupled cavity-array with one deposited  $\Lambda$ -type atom. (b) shows the internal structure of the  $\Lambda$ -type atom along with its coupling light fields, where the red curly line array denotes the quantum light field propagating in the cavity-array and the red arrow denotes the classical light field. (c) shows the cavity-array with two  $\Lambda$ -type atoms deposited at different sites, which forms a secondary cavity.

where  $\Delta = \omega_a - \omega_C$  is frequency detuning between the metastable state and the classical light field or the model's control parameter in the EIT mechanism.

Our setup can be physically implemented in two ways. One is to place artificial  $\Lambda$ -type atoms in the 1D defect cavities of a 2D optical crystals [cite:greenree]. The other is to use an 1D superconducting transmission line of resonators controlled by a three-level Josephson junction. Both the optical crystal line-cavity and the superconducting transmission-line resonators provide the 1D continuum for coherent transport of photons. The controller parts are implemented by an external classical light field in the case of a  $\Lambda$ -atom and an external magnetic field in the case of an artificial Josephson three-level atom.

## III. DISCRETE SCATTERING BY THE THREE-LEVEL FQN

To consider the 1D scattering problem for the above model, we divide  $H^R = H_0 + H_I$  into two parts where  $H_0 = H_p + H'_a$  is the free energy part of the cavity-array and the three-level atom, and  $H_I = H'_c$  is the controlling interaction. Through controlling the Rabi frequency and the cavity mode frequency of the classical field, we can adjust the reflection and the transmission of light through the atom and thus manipulate the propagation of the single photon in the 1D continuum.

The single photon process defines a conversation rule of total occupation number (photons in the cavities plus the excitations of the atom). Written in the tensor product

space, this occupation number operator reads

$$\hat{N} = \sum_j |1_j, g\rangle \langle 1_j, g| + |0, a\rangle \langle 0, a| + |0, e\rangle \langle 0, e| = 1,$$

which commutes with the total Hamiltonian. In above identity,  $|1_j, g\rangle$  represents the state in which a photon occupies the site  $j$  while all other sites  $i \neq j$  have no photon and the atom is at ground state  $|0, e\rangle$  and  $|0, a\rangle$  represent the states in which no photon exists in the cavity-array while the atom is promoted to the excited state and the metastable state, respectively. We hence find an invariant subspace spanned by the stationary eigenvectors

$$|E\rangle = \sum_j u(j) |1_j, g\rangle + u_a |0, a\rangle + u_e |0, e\rangle.$$

where  $u(j)$ ,  $u_a$ ,  $u_e$  denotes the probability amplitudes for each state accordingly.

The eigen-equation  $H|E\rangle = E|E\rangle$  results in the system of equations

$$\begin{aligned} (E - \omega)u(j) &= -tu(j+1) - tu(j-1) + gu_e\delta_{j,0}, & ( \\ (E - \omega_e)u_e &= gu(0) + \Omega u_a, & ( \\ (E - \Delta)u_a &= \Omega u_e, & ( \end{aligned}$$

about the probability amplitudes. By eliminating the amplitudes for the atom's excited state and metastable state, we obtain the discrete scattering equation for the amplitude of the single photon

$$[E - \omega - V(j)]u(j) = -tu(j+1) - tu(j-1), \quad (8)$$

where

$$V(j) = \frac{g^2(E - \Delta)}{(E - \omega_e)(E - \Delta) - \Omega^2} \delta_{j,0} = V\delta_{j,0} \quad (9)$$

is the  $\delta$ -type effective potential determined by the internal structure of the  $\Lambda$ -type atom and  $V$  indicates the magnitude of the potential.

It should be pointed out that the effective potential  $V(j)$  is actually dependent on the eigenenergy  $E$ . Or inversely the energy  $E$  of the incident photon indirectly determines the magnitude of the effective potential and can thus render the effective potential smoothly from a barrier to a well following its variation. Although this scattering potential is not energy-independent, we can still apply the time-independent scattering theory in the coordinate space for some certain energy of the incident photon.

We are interested in the conditions when the total reflection or the total transmission of the photon controlled by an external classical field occur. Under such circumstances, the atom behaves like a single photon switch. When we apply a classical field with a matching frequency, the EIT effect occurs, there is no photon transport in and out of the cavity-array. The physical property

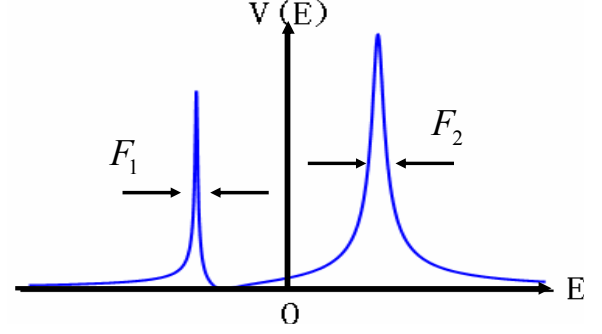


FIG. 2: Schematic diagram of the potential, where we apply two decay rates in order to make the values at resonant frequencies finite.

of the photon transport is totally contained in  $V(j)$ . Its magnitude  $V$  can be rewritten as

$$V = g^2 \left( \frac{A}{E - \omega_+} + \frac{B}{E - \omega_-} \right), \quad (10)$$

where the two peaks of maximum magnitude are defined by the two resonant frequencies

$$\omega_{\pm} = \frac{\omega_e + \Delta}{2} \pm \mu, \quad (11)$$

and the corresponding amplitudes

$$A = \frac{1}{2}(1 + \nu), \quad (12a)$$

$$B = \frac{1}{2}(1 - \nu). \quad (12b)$$

In the above identities,

$$\mu = \sqrt{\Omega^2 + \left( \frac{\omega_e - \Delta}{2} \right)^2} \quad (13)$$

denotes the energy splitting between the two resonant frequencies and

$$\nu = \frac{\omega_e - \Delta}{2\mu}. \quad (14)$$

the amplitude difference between the two peaks. The absolute value of the potential is plotted in Fig. 2, which explicitly shows the two peaks at two different values of energy  $E$ . In order to make the potential finite, we have phenomenologically introduced two additional decay rates  $\Gamma$  and  $\gamma$  for the metastable and the excited states, respectively, of the atom.

The full widths at half maximum are

$$F_1 = \frac{\Gamma + \gamma}{2} - (\Gamma - \gamma)\zeta, \quad (15a)$$

$$F_2 = \frac{\Gamma + \gamma}{2} + (\Gamma - \gamma)\zeta, \quad (15b)$$

which is derived from the first order Taylor's expansion by assuming large quality factors  $\Gamma/\omega_e$  and  $\gamma/\Delta$ .

It is obvious that the scattering of the photon by the  $\Lambda$ -type three-level atomic FQN can be regarded as scattering by two two-level FQN's at the same position. This fact can be seen from the detailed calculation about the transmission and reflection by two-level FQN's in Ref. [15]. The main conclusion is that the FQN play the same role as that of a  $\delta$ -potential in the 1D scattering problem. Tuning the FQN properly can establish an infinite potential barrier to totally reflect the incident single photon. The detailed discussions are given in the next section.

#### IV. CONTROLLABLE REFLECTION AND TRANSMISSION

##### A. The tunable double peak

For the coherent transport of a single photon in the 1D continuum, the scattering equation

$$(E - \omega)u(j) = -tu(j+1) - tu(j-1) \quad (16)$$

for  $j \neq 0$  assumes a usual solution

$$u(j) = \begin{cases} e^{-ikj} + re^{ikj}, & j < 0 \\ se^{-ikj}, & j > 0 \end{cases}, \quad (17)$$

where  $r$  and  $s$  are the reflection and the transmission coefficients, respectively. The cavity lattice constant is normalized to 1. Apparently, the energy  $E$  of the incident photon obeys the dispersion relation

$$E = \omega - 2t \cos(k), \quad (18)$$

dependent on the momentum  $k$  the of incident photon.

The continuous condition  $u(0^+) = u(0^-)$  together with scattering equation at the zeroth site

$$[E - \omega - V]u(0) = -tu(1) - tu(-1) \quad (19)$$

determines the reflection coefficient

$$r = \frac{V}{2it \sin(kl) - V}, \quad (20)$$

and the transmission coefficient  $s = 1 + r$ .

The reflection coefficient for single photon transport is plotted in Fig. 3. The reflection coefficient is plotted against the momentum  $k$  of the incident photon in Fig. 3(a) and Fig. 3(b), and against the energy  $\varepsilon_k = E(k) - \Delta$  in Fig. 3(c) and Fig. 3(d). Obviously, there are rich lineshapes beyond the conventional Breit-Wigner and Fano-Feshbach types.

For a single incident photon with a definite momentum, the potential  $V(j)$  determines all the properties of a scattering process. The potential is only located at

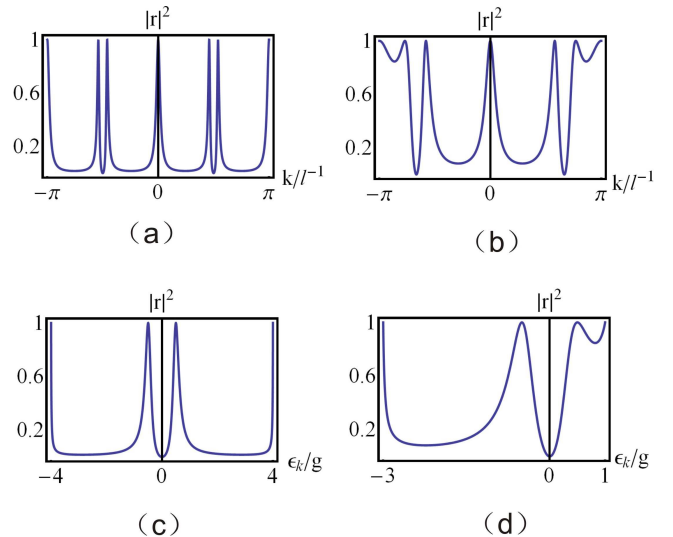


FIG. 3: Reflection coefficients vs.  $k$  and  $\varepsilon_k$ . (a) and (b) is plotted versus momentum  $k$  of incident photon, and (c) and (d) is plotted versus energy  $\varepsilon_k$ . Here the parameters in our setup is chosen as: (1)  $t = 2$ ,  $\omega = 1$ ,  $\omega_e = 1$ ,  $\Delta = 0$ ,  $\Omega = 1$  (all is in units of coupling constant  $g$ ) for (a) and (c); (2)  $t = 1$ ,  $\omega = 1$ ,  $\omega_e = 2$ ,  $\Delta = 0$ ,  $\Omega = 0.75$  (all is in units of coupling constant  $g$ ) for (b) and (d).

the zeroth site where the  $\Lambda$ -type atom is placed. The nontrivial cases

$$r = \begin{cases} 0, & \text{perfect transmission} \\ -1, & \text{perfect reflection} \end{cases} \quad (21)$$

occurs when the potential  $V(j)$  takes special values. The zeros of  $V(j)$  correspond to perfect transmission, and the singularities of  $V(j)$  correspond to perfect reflection. Therefore, we can control reflection and transmission by tuning the Rabi frequency  $\Omega$  and the control field frequency  $\omega_C$ . Similar to the phenomenon of the negative differential electric resistance in an electronic transistor, we observe here a “negative differential photonic resistance”. Following this comparison, we have demonstrated an all-optical device.

From Eq.(9), the energy  $E$  of the single photon at perfect transmission, i.e.  $V = 0$ , satisfies

$$E - \Delta = 0, \quad (22)$$

which is exactly the two-photon resonant condition. The photons scattered from the two potential peaks interfere coherently such that the back traveling photon is eliminated while the forward traveling photon is constructed, which gives perfect transmission to the incident photon. This phenomenon never occurs in 1D scattering problem with a two-level FQN in Ref. [15] because of the lack of the EIT mechanism in a two-level atom. The case of ideal transparency can be easily found in Fig. 3, where in the vicinity of  $\varepsilon_k = 0$  the original single peak in Ref. [15] splits into two peaks. The splitting position can

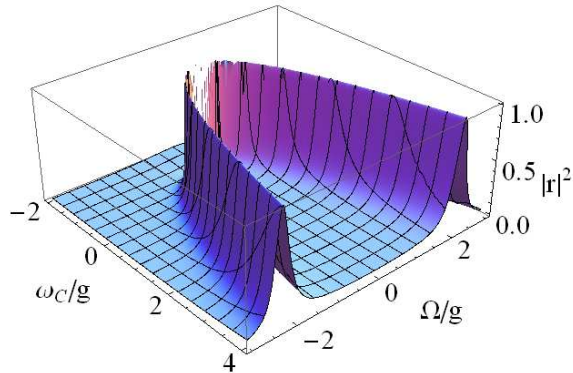


FIG. 4: (Color online) 3D plot of reflection coefficients vs Rabi frequency  $\Omega$  and energy level spacing of classical light field  $\omega_C$  (Both  $\Omega$  and  $\omega_C$  is in units of coupling constant  $g$ ).

be tuned by varying the Rabi frequency of the classical control field.

The other nontrivial case is the perfect reflection, where the three-level atom acts like a perfect “mirror”. The perfect reflection caused by the singularities of the potential  $V$  takes place only when the energy of the incident photon resonates with one of the internal level spacings of the three-level atom.

In Fig. 4, we can see how the reflection coefficient varies with the Rabi frequency  $\Omega$ , as the x-axis, and with the frequency  $\omega_C$  of the external control field, as the y-axis. The existence of the double peaks in the plot shows that when fixing one of the parameters  $\Omega$  or  $\omega_C$ , we can always fine tune the other parameter to reach perfect reflection or transmission. The reason why there always exist two peaks for perfect reflection is that the  $\Omega^2$  term in the reflection coefficient corresponds to two values,  $\Omega$  and  $-\Omega$ , of the Rabi frequency.

The high and the low energy limits are obtained in the vicinity of  $k = \pi/2$  and  $0$ , respectively. The reflection coefficients become ( $h$  and  $l$  index the high and the low energy limits, respectively)

$$r = \begin{cases} V_h/(2it - V_h), & (k \rightarrow \pi/2) \\ V_l/(2itk - V_l), & (k \rightarrow 0) \end{cases}, \quad (23)$$

where the corresponding potentials in the high and the low energy limits equal to

$$V_m = \frac{g^2 \varepsilon_m}{(\Delta \varepsilon_m + \Delta - \omega_e) \varepsilon_m - \Omega^2}, \quad (m = h, l). \quad (24)$$

The reflection coefficient is plotted against the energy  $\varepsilon_m$  in Fig. 5: (a) in the high energy limit as a function of  $\varepsilon_h$  where the energy obeys the linear dispersion relation  $\varepsilon_h = (\omega - t\pi - \Delta) + 2tk$ , and (b) in the low energy limit as a function of  $\varepsilon_l$  where the energy obeys the quadratic dispersion relation  $\varepsilon_l = (\omega - 2t - \Delta) + tk^2$ . Obviously, the lineshapes are different from the conventional Breit-Wigner and Fano-Feshbach types.

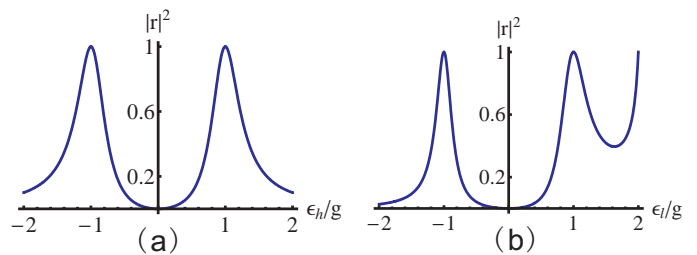


FIG. 5: The reflection coefficients as functions of  $\varepsilon_m$  are plotted under (a) the high energy limit and (b) the low energy limit. None of the lineshapes are simple Breit-Wigner and Fano-Feshbach types.

## B. Equivalence to a pair of two-level atoms

To show explicitly that the three-level FQN is equivalent to a pair of two-level atoms placed apart in the cavity-array, we consider the scattering problem in the 1D continuum with one two-level atom deposited at the zeroth site and the other at the  $D$ -th site. By a similar approach in discrete coordinate representation used in Ref.[zhou], we obtain the reflection and the transmission coefficients

$$r = \frac{V_1 f_2(k) \exp(i2kD) - V_1 V_2 + V_2 2t i \sin k}{-f_1(k) f_2(k) \exp(i2kD) + V_1 V_2}, \quad (25a)$$

$$s = \frac{(2t \sin k)^2 \exp(i2kD)}{-f_1(k) f_2(k) \exp(i2kD) + V_1 V_2}, \quad (25b)$$

where the transport functions are defined

$$f_m(k) = 2si \sin k + V_m, \quad (m = 1, 2) \quad (26)$$

with the potentials

$$V_m = \frac{g_m^2}{E - \omega_m}, \quad (m = 1, 2). \quad (27)$$

The reflection and the transmission coefficients in Eqs.(25a) and (25b) are identical to the ones in our setup, besides the additional phase factor  $\exp(i2kD)$  determined by the momentum  $k$  of the incident photon and the distance  $D$  between the two FQN's. We observe that the effect of  $D$  is totally contained in this phase factor, which equals to the phase difference between the incident wave and the reflected wave from the  $D$ -th site. The two effective potentials in Eq.(27) together play the same role as the complex potential in Eq.(9). If we treat the two atoms with the cavities in between as an extended “FQN”, then for a certain momentum  $k$  of incident photon, the phase factor becomes  $\exp(i2kD) = 1$  and this extended “FQN” is equivalent to a  $\Lambda$ -type atom in our setup.

For a fixed distance  $D$ , the transmission and the reflection coefficients are plotted in Fig. 6(a). In this setup, the perfect reflection can be attained when both the effective potentials  $V_1$  and  $V_2$  tend to infinity. However,

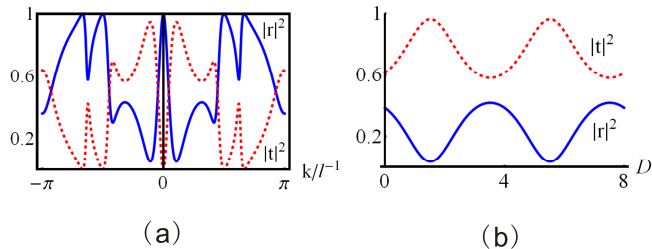


FIG. 6: (Color online) (a) The reflection and the transmission coefficients vs.  $k$  for two distant two-level FQN's. (b) The reflection and the transmission coefficients vs.  $D$  for two distant two-level FQN's. Blue solid and red dashed line represent reflection and transmission coefficients, respectively.

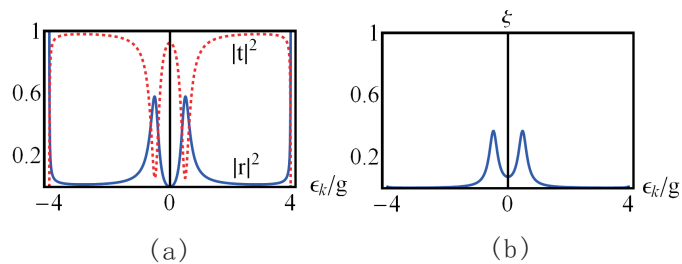


FIG. 7: Reflection coefficients and the energy loss ratio vs.  $\epsilon_k$ , respectively in (a) and (b). Here the parameters in our setup is chosen as:  $t = 2$ ,  $\omega = 1$ ,  $\omega_e = 1$ ,  $\Delta = 0$ ,  $\Omega = 1$ ,  $\gamma = \Gamma = 0.04$  for both (a) and (b) (all is in units of coupling constant  $g$ ) (all is in units of coupling constant  $g$ ) for (b).

the existence of perfect transmission is not guaranteed. Not only the two-photon resonance condition but also the distance constrain  $\exp(i2kD) = 1$  must be met to attain perfect transmission. For a fixed momentum  $k$ , the periodic variance of the transmission and the reflection coefficients is shown in Fig. 6(b).

### C. Cavity decay and atomic decay

The material and devices imperfections result in unavoidable energy relaxation and dephasing of devices. Such a decoherence effect results in the inelastic scattering of a single photon and reduce the switching efficiency.

For atomic decay, it can be simply demonstrated by phenomenologically introducing two additional atomic decay rates  $\Gamma$  and  $\gamma$  for the metastable and the excited states, respectively, of the atom. According to the Eqs. (15a) and (15b), the maximum value of effective potential is decreased to a finite value, which implies that perfect reflection would not be obtained any more.

To derive the scattering property of the propagation of a single photon with atomic decays  $\Gamma$  and  $\gamma$ , the frequencies  $\omega_e$  and  $\Delta$  are substituted by  $\omega_e - i\Gamma$  and  $\Delta - i\gamma$  to phenomenologically represent the atomic energy relaxation. The straightforward calculation gives the re-

flexion amplitude as

$$r = \frac{V_d}{2it \sin(kl) - V_d}, \quad (28)$$

where

$$V_d = \frac{g^2(E - \Delta + i\gamma)}{(E - \omega_e + i\Gamma)(E - \Delta + i\gamma) - \Omega^2} \quad (29)$$

and the corresponding transmission amplitude  $s = 1 + r$ . The reflection coefficient for single photon transport with atomic decay is plotted in Fig. 7 (a).

Obviously, the perfect transparency can not be obtained even when the absolute value of effective potential is zero. The maximum value of transmission coefficient is less than 1 depicted in Fig. 7(a). At the meantime, the maximum value of reflection coefficient depicted as peaks in Fig. 7(a) are dramatically decreased. And the summation of reflection coefficient and transmission coefficient is always less than 1, which implies that the single photon undergo an inelastic scattering process. This inelastic effect is plotted in Fig. 7 (b). The label of y-axis  $\xi = 1 - (|r|^2 + |t|^2)$  represents the ratio of loss energy after the inelastic scattering.

To depict the non-ideal scattering process with various decoherences, we need to consider the coherent length (CL) of the scattering process, and an infinite CL means an ideal elastic scattering. Here, the CL can be regarded as the distance that the photon travels between the left side and the right side of the scatterer (the three-level system). Actually, to make sure that the scattering process can happen, it is required that the photon leakage rate  $\kappa$  for each resonator is much smaller than the hopping constant, otherwise photons will totally escape into the environment before encountering the scatterer. Therefore, we think that the photon leakage rate  $\kappa$  defines the CL, which is roughly proportional to the product of  $\kappa^{-1}$  and the group velocity of the photons. Moreover, any additional change of the leakage rate, at the point where the scatterer is located, will broaden the width of the lineshape at the resonance (i.e., there is a peak at the transition energy).

To study in detail, this decoherence effect, we need to use a microscopic model where both the cavities and the there-level system are coupled to the external environment. The decoherence of every cavity and the there-level system mainly results in the incoherent or dissipative propagation of the incident photon. In such approach, the decoherence or dissipation can be divided into two categories according to its contributions to the scattering process. One category contains all the cavity decays, except the one of the cavity which is directly coupled to the there-level system, since these resonators contribute to the free propagation of the photon. This trivial type of photon leakage rate in each cavity only affects the coherent length of the scattering process. The other category influencing the scattering process contains the decay of the there-level system and the decay of the

cavity directly coupled to the two-level system. Because the energy of the incident photon is not conservative before and after the scattering happens, the scattering is obviously inelastic. The inelastic scattering process would broaden the width of the lineshape. These different decoherence categories would reduce the quantum switching efficiencies in different ways.

## V. FORMING A SECONDARY CAVITY WITH TWO FQN'S

According to the results derived above, we now propose a controllable secondary cavity architecture. We place two  $\Lambda$ -type FQN's at the zeroth site and the  $D$ -th site in the 1D cavity-array (Fig. 1(c)). These two FQN's acting as  $\delta$ -potentials with tunable potential are controlled by external classical light fields. The most natural consideration is that there exists a quasibound state between the two  $\delta$ -potentials, which can degenerate to become a bound state under some special cases. In our setup, it is intuitive that the two  $\Lambda$ -type FQN's form a secondary cavity for single photon storage among the regular cavities in the array. We can prove that only incident photons of some particular momenta can be stored in this secondary cavity.

The total Hamiltonian in the "rotating" frame of reference

$$H^R = H_p + H'_a + H'_c \quad (30)$$

reads

$$H_p = \sum_j [\omega b_j^\dagger b_j - t(b_j^\dagger b_{j+1} + h.c.)], \quad (31)$$

$$H'_a = \sum_{l=1,2} [\omega_{e,l} |e\rangle \langle e_l| + \Delta_l |a\rangle \langle a_l|], \quad (32)$$

$$H'_c = \sum_{l=1,2} [\Omega_l (|a\rangle \langle e_l| + h.c.) + g_l (b_l^\dagger |g\rangle \langle e_l| + h.c.)] \quad (33)$$

where  $H_p$  describes the free energy of the photon,  $H'_a$  the potential energy of the two FQN's with detunings  $\Delta_l = \omega_{a,l} - \omega_{C,l}$  ( $l = 1$  indicates the FQN at the zeroth sites while  $l = 2$  that of the  $D$ -th site), and  $H'_c$  the interaction of the FQN's with the photon probe and the classical control fields.

Again, the energy eigenvectors can be expanded in the basis of an invariant subspace in the form

$$|E\rangle = \sum_j u(j) b_j^\dagger |0, g, g\rangle + \sum_{l=1,2} [u_a^l |0, a, g\rangle + u_e^l |0, e, g\rangle], \quad (34)$$

where  $u(j)$  is the probability amplitude of the single photon at the  $j$ -th site. Following the same procedure as in the one FQN case, we obtain the scattering equation of the probability amplitudes

$$[E - \omega - \sum_{l=1,2} V_l \delta_{j,l}] u(j) = -t u(j-1) - t u(j+1), \quad (35)$$

where the potentials at the two sites of FQN's are

$$V_l = \frac{g_l^2 (E - \Delta_l)}{(E - \omega_{e,l})(E - \Delta_l) - (\Omega_l)^2}, \quad (l = 1, 2). \quad (36)$$

It should be noted that both the potentials act like  $\delta$ -potentials, between which a quasibound state can survive.

The quasi-bound state can be considered the analytic continuation of a scattering state into the complex momentum plane singular reflection and transmission coefficients. Accordingly, we first assume the scattering state to be

$$u(j) = \begin{cases} e^{-ikjl} + r e^{ikjl}, & j < 0 \\ s_1 e^{-ikjl} + r_1 e^{ikjl}, & 0 < j < D, \\ s e^{-ikjl}, & j > D \end{cases} \quad (37)$$

where  $r$  and  $s_1$  are the reflection and the transmission coefficients at the zeroth site, whereas  $r_1$  and  $s$  are those at the  $D$ -th site. Since we are only interested in the effective behavior of the secondary cavity as an intact storage device, the intra-cavity analysis of wave transmission can be neglected. That is, we are only concerned about the coefficients  $r$  and  $s$  viewed from outside the secondary cavity, whose values are the solution of the boundary value problem Eq.(37) and read

$$r = \frac{V_1 f_2(k) \exp(i2kD) - V_1 V_2 + V_2 2t \sin k}{-f_1(k) f_2(k) \exp(i2kD) + V_1 V_2}, \quad (38a)$$

$$s = \frac{(2t \sin k)^2 \exp(i2kD)}{-f_1(k) f_2(k) \exp(i2kD) + V_1 V_2}. \quad (38b)$$

Except that the potentials  $V_1$  and  $V_2$  are defined as in Eq.(36), the above expressions are identical to Eq.(25a) and Eq.(25b), which leads to perfect transmission through the secondary cavity based on EIT mechanism.

The quasi-bound state then occurs when the denominators of the two coefficients equal to zero, which corresponds to the condition

$$e^{i2kD} = \frac{V_1 V_2}{(2t \sin k + V_1)(2t \sin k + V_2)}, \quad (39)$$

from which the momentum  $k$  of a single photon surviving between the potentials  $V_1$  and  $V_2$  is determined. The incident photon corresponding to this intra-cavity photon has its momentum take imaginary values, which in turn leads to its imaginary energy. The imaginary energy will result in a decay of the wavefunction, which means the quasi-bound state is a bound state with a small leakage at two ends. When  $\omega \gg t$ , it is almost impossible for a single photon to propagate in the channel and quasi-bound states are formed in the secondary cavity.

The most interesting quasi-bound state can be obtained when both FQN's are tuned to their resonant states, where

$$e^{-i2kDl} = 1. \quad (40)$$

The above formula subjects the momentum of the trapped photon to a quantized value

$$k = \frac{\pi n}{Dl}, \quad (41)$$

where  $n$  is an arbitrary integer. The corresponding bound state is

$$u(j) = \begin{cases} 0, & j < 0 \text{ or } j > D \\ A \sin(kj), & 0 < j < D \end{cases} \quad (42)$$

where  $A$  is the normalization constant. So the incident photon can be perfectly trapped between the two FQN's, similar to what happens in a single cavity. We hence name this setup a perfect secondary cavity, which realizes a non-destructive single photon storage.

Compared to the proposals of quantum memories based on the dark state in the EIT effect, our secondary cavity setup is much easier to implement. In the former, the dark state is stationary and the classical field is adiabatically manipulated to store information from the incident photon to the three-level atom. Such a process should be regarded as a stationary storage and demands highly precise control over the external control field. Whereas, the secondary cavity proposed here is dynamic and the control parameters, including the distance  $D$  between the FQN's, the Rabi frequency  $\Omega$ , and the frequency  $\omega_C$  of the external field, are all much easier to manipulate. The storage process can be imagined as disposing two perfectly reflecting "mirrors" in the cavity-array such that a single photon originally traveling in the array is bounded in between to become a standing wave. The releasing process is to inversely remove these two reflecting "mirrors".

## VI. CONCLUSION

We have revisited the problem of single photon transport in an 1D cavity-array with a deposited three-level

$\Lambda$ -type FQN and illustrated how the reflection and the transmission coefficients rely on the Rabi frequency and the traveling frequency of a classical control field external to the cavity array. By tuning these two frequencies, the FQN can serve as a perfect "mirror" or a transparent medium for an incident photon. The appearance of line-shapes different from the conventional Breit-Wigner or Fano-Feshbach type was shown to stem from a nonlinear dispersion relation and the EIT mechanism in the setup.

The dissipation of cavities and atom are taken into account. The atomic decay is added phenomenologically to explain the single photon undergo an inelastic scattering process. The cavities decay mainly determine the coherent length, which limit the upper number of cavities.

Using this phenomenon, we have proposed a secondary cavity between two FQN's, in which a controllable quasi-bound state can be formed, to coherently store a single photon. A perfect secondary cavity selects photons with momenta being integral multiples of a constant. The limiting lossless case has also been presented to compare with the usual photon storage using an EIT dark state.

## Acknowledgments

The authors thank H. Dong, T. Shi and D. Z. Xu for helpful discussion. This work is supported by the NSFC with Grants No.90203018, No.10474104, No.60433050 and No. 10704023. It is also funded by the National Fundamental Research Program of China with Grants No.2001CB309310 and No.2005CB724508.

- 
- [1] P. Bermel, A. Rodriguez, S. G. Johnson, J. D. Joannopoulos, and M. Soljačić, *Phys. Rev. A* **74**, 043818 (2006).
  - [2] D. E. Chang, A. S. Sørensen, E. A. D. and M. D. Lukin, *Nature Phys.* **3**, 807 (2007).
  - [3] M. Orrit, *Nature Phys.* **3**, 755 (2007).
  - [4] M. Hijlkema, B. Weber, H. P. Specht, S. C. Webster, A. Kuhn, and G. Rempe, *Nature Phys.* **3**, 253 (2007).
  - [5] M. J. Werner, and A. Imamoglu, *Phys. Rev. A* **61**, 011801(R) (1999).
  - [6] S. Rebic, S. Tan, A. Parkins, and D. Walls, *J. Opt. B: Quantum Semiclassical Opt.* **1**, 490 (1999).
  - [7] K. M. Gheri, W. Alge, and P. Grangier, *Phys. Rev. A* **60**, R2673 (1999).
  - [8] A. D. Greentree, J. A. Vaccaro, S. R. de Echaniz, A. V. Durrant, and J. P. Marangos, *J. Opt. B: Quantum Semiclassical Opt.* **2**, 252 (2000).
  - [9] K. Birnbaum, A. Boca, R. Miller, A. Boozer, T. Northup, and H. J. Kimble, *Nature (London)* **436**, 87 (2005).
  - [10] A. G. White, P. K. Lam, D. E. McClelland, H. A. Bachor, and W. J. Munro, *J. Opt. B: Quant. Semiclass. Opt.* **2**, 553 (2000).
  - [11] R. Ruskov, K. Schwab, and A. N. Korotkov, *IEEE Trans. Nanotechnol.* **4**, 132 (2005).
  - [12] R. Almog, S. Zaitsev, O. Shtempluck, and E. Buks, *Phys. Rev. Lett.* **98**, 078103 (2007).
  - [13] B. Yurke and E. Buks, *J. Lightwave Technol.* **24**, 5054 (2006).
  - [14] A. B. Klimov, L. L. Sánchez-Soto, and J. Delgado, *Opt. Comm.* **191**, 419 (2001).
  - [15] Lan Zhou, Z. R. Gong, Yu-xi Liu, C. P. Sun, and Franco Nori, *Phys. Rev. Lett.* **101**, 100501 (2008).

- [16] Jung-tsung Shen and Shanhui Fan, *Opt. Lett.* **30**, 2001 (2005).
- [17] Jung-tsung Shen and Shanhui Fan, *Phys. Rev. Lett.* **95**, 213001 (2005).
- [18] Jung-tsung Shen and Shanhui Fan, *Phys. Rev. Lett.* **98**, 153003 (2007).
- [19] N. Hatano, K. Sasada, H. Nakamura and T. Petrosky, *Prog. Theor. Phys.* **119**, 187 (2008).
- [20] H. Nakamura, N. Hatano, S. Garmon and T. Petrosky, *Phys. Rev. Lett.* **99**, 210404 (2007).